Recombination at dangling bonds and steady-state photoconductivity in a-Si:H

F. Vaillant and D. Jousse

Laboratoire d'Etudes des Propriétés Electroniques des Solides, Centre National de la Recherche Scientifique, B.P. 166, 38042 Grenoble Cédex, France

(Received 26 February 1986)

A simple model of recombination at dangling bonds in a-Si:H is proposed to explain the steady-state photoconductivity and γ-exponent variations with the equilibrium Fermi-level position. The appropriate statistics for correlated defects and the Shockley-Read formalism are used to obtain a parametrical representation of photoconductivity versus optical generation rate. Oscillations of γ between 0.5 and 1 when E_F is shifted in the central region of the gap depend mainly on the density of dangling bonds and the energy positions of the singly (T_3^0) and doubly (T_3^-) occupied levels. Experimental results on lightly-boron-doped glow-discharge a-Si:H are in agreement with the model and give a location of the T_3^0 level at 0.95 eV from E_c, an effective correlation energy of 0.4 eV, and a ratio of charge-to-neutral-state capture cross sections of 50. Finally, the dangling-bond-state occupation probabilities are shown to be weakly modified by illumination even at high photon fluxes. Consequences for the interpretation of ESR experiments are also discussed.

I. INTRODUCTION

The dangling-bond (DB) center plays an essential role in the recombination of excess carriers in hydrogenated amorphous silicon (a-Si:H) because of its amphoteric nature and its location in energy around midgap. This has been assessed from steady-state and transient experiments, such as photoluminescence,[1,2] electron-spin resonance[3] (ESR), and optically detected magnetic resonance[4] (ODMR). It has been confirmed by the fact that the mobility-lifetime products for excess carriers are inversely proportional to the density of dangling-bond centers.[5,6] The peculiarity of this defect is that, at equilibrium, it may be neutral (T_3^0), or positively (T_3^+) or negatively (T_3^-) charged according to the position of the Fermi level E_F. From ESR studies on undoped and doped a-Si:H, the effective correlation energy E_U was shown to be positive[7,8] and the influence of the correlation effect on the electronic properties of a-Si:H was first outlined by Schweitzer *et al.*[9]

In spite of this, most of the experimental results on steady-state photoconductivity have been interpreted through two models that consider trapping and recombination of excess carriers via gap states which are not correlated.[10] Anderson and Spear[11] reported that the exponent of the illumination power dependence, γ, changed from 1.0 to 0.5 when E_F was shifted by phosphorous doping. The effect was attributed to a progressive transition from monomolecular to bimolecular kinetics due to a changing occupation of the so-called E_y peak in the density of states (DOS) deduced from field-effect experiments. The γ values intermediate between 1.0 to 0.5 commonly obtained in a-Si:H (Refs. 12—14) were better explained on the basis of Rose's model[15] which predicts, for an exponentially distributed DOS, $\gamma=E_0/(E_0+k_BT)$ where E_0 is the characteristic energy of the majority-carrier band tail. More recently, Hack *et al.*[16] have interpreted the dependence of γ on Fermi-level position by introducing four exponential distributions in the gap DOS.

The occupancy of the different DB states follows the statistics of correlated electrons instead of Fermi-Dirac statistics. Exact knowledge of the occupation rates under illumination is of prime importance in order to interpret photoconductivity measurements and also ESR experiments under lightlike quenching of ESR, or light-induced ESR (LESR). Some photoconductivity characteristics have been recently derived by Okamoto *et al.*[17] for recombination at DB's under particular conditions.

The photoconductivity model presented here treats without approximations and at all illuminations the case of steady-state photoconductivity controlled by the recombination at DB's and trapping at band tails. The error induced by the usual approximation of uniform generation along thickness is evaluated.

A short review of the case of recombination at a single level will introduce the model itself which is described in Sec. II along with the basic equations. The choice of parameters and calculation results are given in Sec. III. A discussion follows in Sec. IV where theoretical predictions are compared to our own experimental γ versus E_F data obtained on boron-doped glow-discharge a-Si:H and to other published results.

II. THEORY

A. Single recombination center: review and results

We first recall the basic equations describing the recombination of free carriers through a single recombination center at energy E_t of density N_t per unit volume and deduce the variation of the exponent γ with the equilibrium Fermi level.

According to Shockley-Read statistics,[18] the recombination rates for electrons and holes, U_n and U_p are (cf. Fig. 1)

$$U_n=v_n\sigma_n[nN_t(1-f_t)-n_1N_tf_t]\ ,\qquad(1)$$

 ©1986 The American Physical Society

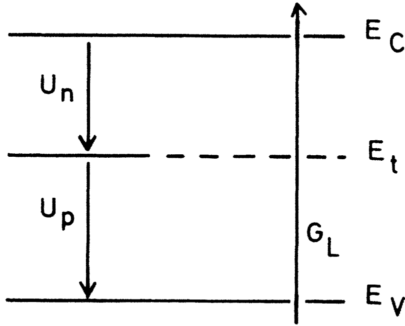

FIG. 1. Representation of the electron flows in the simplified model of one recombination level.

$$U_p = v_p \sigma_p [p N_t f_t - p_1 (1-f_t)] , \quad (2)$$

where v_n and v_p are the thermal velocities of electrons and holes and σ_n and σ_p are the capture cross sections of the center for electrons and holes. The thermal occupation rate of the center by an electron ft_0 is

$$ft_0 = \frac{1}{1+\exp[\beta(E_t - E_F)]} \quad (3)$$

with $\beta = 1/k_B T$; n and p are the free-electron and free-hole densities; n_1 and p_1 are, respectively, defined by

$$n_1 = n_i \exp[\beta(E_t - E_i)] , \quad (4)$$

$$p_1 = n_i \exp[\beta(E_i - E_t)] , \quad (5)$$

with n_i the intrinsic concentration and E_i the intrinsic level defined as the middle of the gap as in classical semiconductor theory.

In the steady state $U_n = U_p = G_L$ where G_L is the number of photogenerated electron-hole pairs per unit volume and per second. We obtain

$$f_t = \frac{v_n \sigma_n n + v_p \sigma_p p_1}{v_n \sigma_n (n + n_1) + v_p \sigma_p (p + p_1)} \quad (6)$$

and deduce

$$G_L = \frac{v_n \sigma_n v_p \sigma_p N_t (np - n_i^2)}{v_n \sigma_n (n + n_1) + v_p \sigma_p (p + p_1)} . \quad (7)$$

Using electrical charge conservation

$$n - p + N_t f_t = n_0 - p_0 + N_t ft_0 , \quad (8)$$

where the subscript 0 indicates thermal equilibrium, we obtain a quadratic equation in n and p. Solving this for n as a function of p, Eq. (7) is transformed to yield a parametric representation of the variation of the photoconductivity σ_{ph} with the photogeneration rate:

$$G_L = G_L(p) , \quad (9)$$

$$\sigma_{ph} = q[\mu_n n(p) + \mu_p p] - q(\mu_n n_0 + \mu_p p_0) , \quad (10)$$

where μ_n and μ_p are the free-electron and free-hole mobilities. The exponent γ defined by

$$\sigma_{ph} = K G_L^{\gamma} \quad (11)$$

is obtained from the parametric representation with the help of a computer. The effect of film thickness on measured σ_{ph} is taken into account through the expression given in the Appendix.

This model implicitly neglects the trapping of carriers. It will be shown in Sec. II B that shallow trapping has indeed little effect on γ for E_F close to midgap.

Examples of applications are given in Figs. 2 and 3. In a first step, values of p are chosen to allow variations of G_L between 10^{16} and 10^{20} $cm^{-3}s^{-1}$ that is in the usual experimental range. The variations of σ_{ph} with G_L are given in Fig. 2 for one position of the equilibrium Fermi level and parameters that could be appropriate for hypothetical recombination centers with the same energy levels for the positively-, neutral-, and negatively-charged states (i.e., $E_U \ll k_B T$). Here, σ_n and σ_p are of the order of 10^{-12} cm^2 corresponding to Coulombic centers. The N_t density is around 10^{15} cm^{-3} and the energy level at E_i. Other quantities enter the model with fixed values that will be discussed in Sec. II B 1. In most cases, relation (11) is satisfied in the whole G_L range leading to a well-defined exponent γ. In other cases, a local γ is calculated at $G_L = 10^{19}$ cm^{-3} s^{-1} which corresponds to a photon flux of $\sim 10^{15}$ cm^{-2} s^{-1} at 2 eV. It is now possible to proceed with the calculation in order to obtain the γ values as a function of equilibrium Fermi-level position, as shown in Fig. 3 for a few sets of N_t, σ, and E_t values.

It is worth noting that the exponent γ takes either the value of 0.5 or 1 according to the position of E_F in relation to the energy level E_t with rather sharp transitions between the two plateau regions. The width of the $\gamma = 1$ plateau corresponding to E_F positions around E_t increase with the density of recombination centers [Fig. 3(a)] and their capture cross sections [Fig. 3(b)].

As a matter of fact, an approximate solution of Eqs. (1)–(11) may be derived under the following assumptions:

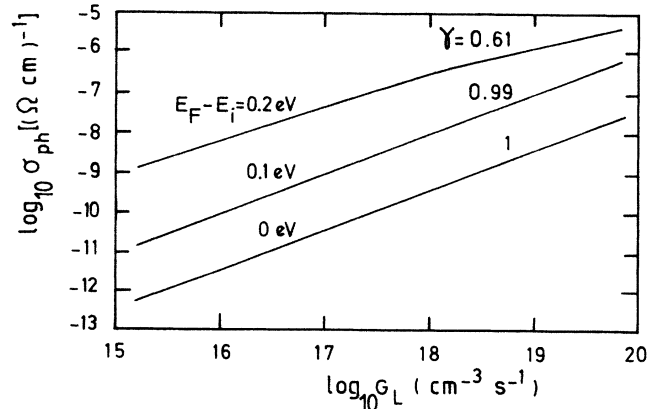

FIG. 2. Dependence of photoconductivity on photogeneration rate for a single recombination level at E_i, $N_t = 10^{15}$ cm^{-3}, $\sigma_n = \sigma_p = 10^{-12}$ cm^2, and three positions of E_F. Indicated are the γ values at $G_L = 10^{19}$ $cm^{-3}s^{-1}$.

(i) the injection of excess carriers is sufficient to verify $n_0 \ll \Delta n$, $p_0 \ll \Delta p$; (ii) E_t situated at or near E_i. In this situation, when electrons are majority carriers, the electron lifetime is given by

$$\tau_n = \tau_{n_0}\left[1 + \frac{\Delta n N_t f_{t_0}}{\Delta n^2 + \Delta n N_t (1 - f_{t_0})}\right] \tag{12}$$

with

$$\tau_{n_0} = 1/v_n \sigma_n N_t \ . \tag{13}$$

An equivalent expression may be derived for the hole

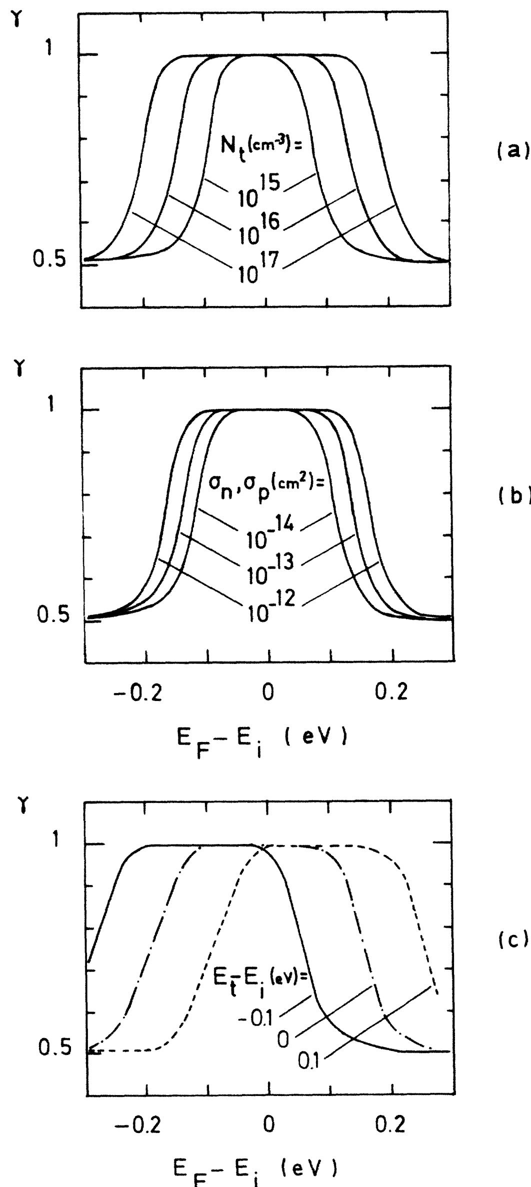

FIG. 3. Variations of the photoconductivity exponent versus E_F for (a) a single recombination level at different densities, (b) capture cross sections, and (c) E_t positions.

lifetime for the case of p-type photoconductivity and it is easy to deduce from (12) that the transitions from $\gamma = 1$ to $\gamma = 0.5$ occur at E_F positions given by

$$E_t + k_B T \ln\left[\frac{N_t}{\Delta n}\right] \text{ and } E_t - k_B T \ln\left[\frac{N_t}{\Delta p}\right]$$

for n- and p-type photoconductivity, respectively.

Although this simple description of the recombination level is known to be unrealistic for most of the a-Si:H materials currently deposited, the reported experimental variations of γ versus E_F (Refs. 11, 13, 16, 19, and 20) can easily be fitted by one of the theoretical curves obtained from this model (see Fig. 3) and have been interpreted by a variety of gap density-of-states distribution: a field-effect-derived DOS,[11] one defect level, and two exponential tails,[13] four exponential tails,[16] and two discrete levels associated with the dangling-bond center.[19] It follows that the values or the variations of the exponent γ alone cannot be used as evidence for a particular DOS distribution. However, the theoretical study of steady-state photoconductivity may help to derive some recombination parameters (energy levels, density, capture cross sections) of an otherwise determined DOS.

Although more complicated, the more realistic case of two correlated levels associated with the dangling-bond center can be handled without approximations using a similar parametric representation for the γ calculation, as demonstrated in the next section.

B. Recombination at dangling bonds and shallow trapping

The most generally accepted DOS for undoped or lightly doped a-Si:H includes two exponential band tails arising from the disorder of the continuous random network and the DB states situated around midgap.[21] Provided the band-tail characteristic energies are sufficiently small (steep tails) as in device-grade glow-discharge a-Si:H (50 and 25 meV for valence-band and conduction-band tails respectively[22]), the tail states and DB states are well separated in energy and can be resolved by deep-level transient spectroscopy (DLTS)[23,24] or photothermal deflexion spectroscopy (PDS).[25]

Under illumination, tail states act as trapping centers and DB states as recombination centers. We shall take the usual assumption that dangling bonds can capture only mobile free carriers. Carrier trapping is expected to have little influence on the recombination kinetics because of the rapid exchange between the shallow traps and the bands. Thus, for the sake of simplicity the continuum of band-tail traps has been replaced by two discrete shallow levels, one for electrons and one for holes. This description agrees with most of the drift-mobility results showing well-defined activated mobilities for both electrons and holes and is adequate for our purpose as long as the Fermi level does not enter the band tails.

The flows of carriers through traps and DB levels may be represented as in Fig. 4. Neither the direct emissions and recombinations nor the transitions between two DB states have been considered. If the density of dangling bonds N_T is not too high, the mean distance between two

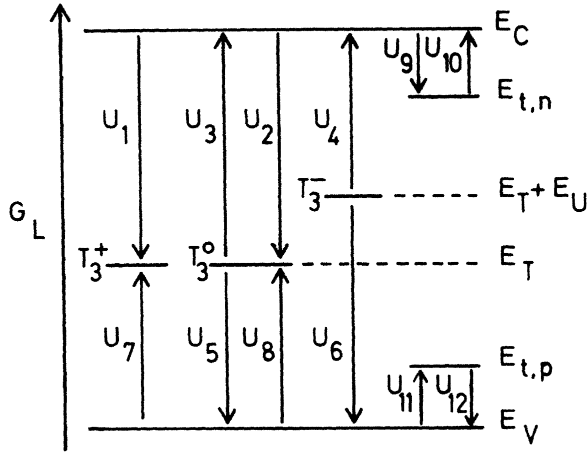

FIG. 4. Schematic representation of the electron flows for shallow trapping and recombination at positively correlated dangling bonds.

localized states is great ($d > 300$ Å for $N_T = 10^{16}$ cm^{-3}) and transitions of the type

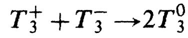

$$T_3^+ + T_3^- \to 2T_3^0$$

have very small probabilities.

The allowed transitions are between dangling bonds and valence or conduction bands given by

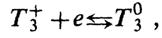

$$T_3^+ + e \leftrightarrows T_3^0 \ ,$$

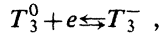

$$T_3^0 + e \leftrightarrows T_3^- \ ,$$

as well as hole or electron trapping. The width of the energy distributions at E_T and $E_T + E_U$ have been neglected for the sake of simplicity. We shall use the following notations: f^+, f^0, and f^- are the occupation rates of DB's in, respectively, the T_3^+, T_3^0, and T_3^- states and f_0^+, f_0^0, and f_0^- are the same rates at thermal equilibrium; c_n^+ and c_n^0 are the electron capture coefficients of T_3^+ and T_3^0, and c_p^0 and c_p^- are the hole capture coefficients of T_3^0 and T_3^-; e_n^0 and e_n^- are the electron emission coefficients of T_3^0 and T_3^-, and e_p^+ and e_p^0 are the hole emission coefficients of T_3^+ and T_3^0; $E_{t,n}$ and $E_{t,p}$ are the energy levels of the electron and hole traps of densities $N_{t,n}$ and $N_{t,p}$; f_n and f_p are the occupation rates of the occupied electron and hole traps; f_n^0 and f_p^0 are the same rates at equilibrium; c_n, e_n, c_p, and e_p are the emission and capture coefficients for the electron and hole traps, respectively.

In the dark, at thermal equilibrium, three independent equations of conservation characterize the system represented in Fig. 4:

$$\frac{dn}{dt} = U_1 - U_3 + U_2 - U_4 = 0 \ , \tag{14}$$

$$\frac{dp}{dt} = U_7 - U_5 + U_8 - U_6 = 0 \ , \tag{15}$$

$$\frac{d[T_3^+]}{dt} = U_1 + U_7 - U_3 - U_5 = 0 \ . \tag{16}$$

The different flows are linked to the concentrations of carriers and recombination centers by the Shockley-Read expressions

$$\begin{aligned} &U_1 = nN_T f^+ c_n^+ , \quad U_5 = N_T f^0 p c_p^0 , \quad U_9 = nN_{t,n}(1-f_n)c_n \ , \\ &U_2 = nN_T f^0 c_n^0 , \quad U_6 = N_T f^- p c_p^- , \quad U_{10} = N_{t,n} f_n e_n \ , \\ &U_3 = N_T f^0 e_n^0 , \quad U_7 = N_T f^+ e_p^+ , \quad U_{11} = pN_{t,p} f_p c_p \ , \\ &U_4 = N_T f^- e_n^- , \quad U_8 = N_T f^0 e_p^0 , \quad U_{12} = N_{t,p}(1-f_p) e_p \ . \end{aligned} \tag{17}$$

Contrary to the one-level model, these equations are not sufficient to determine the thermal emission rates as functions of the capture rates and initial conditions. The principle of detailed balance[26] is required: each charge state of the DB's must be in equilibrium with the band states. So $U_1 = U_3, U_2 = U_4, U_5 = U_7, U_6 = U_8$, and consequently,

$$\begin{aligned} &e_n^0 = n_0 \frac{f_0^+}{f_0^0} c_n^+ , \quad e_n^- = n_0 \frac{f_0^0}{f_0^-} c_n^0 \ , \\ &e_p^0 = p_0 \frac{f_0^-}{f_0^0} c_p^- , \quad e_p^+ = p_0 \frac{f_0^0}{f_0^+} c_p^0 \ . \end{aligned} \tag{18}$$

Using the grand partition function of the system, f_0^+, f_0^0, f_0^- can be easily determined:[27,9]

$$\begin{aligned} &f_0^+ = \frac{1}{1 + 2\exp[\beta(E_F - E_T)] + \exp[\beta(2E_F - 2E_T - E_u)]} \ , \\ &f_0^0 = \frac{2\exp[\beta(E_F - E_T)]}{1 + 2\exp[\beta(E_F - E_T)] + \exp[\beta(2E_F - 2E_T - E_u)]} \ , \\ &f_0^- = 1 - f_0^+ - f_0^0 \ . \end{aligned} \tag{19}$$

The variations of f_0^+, f_0^0, and f_0^- as a function of E_F are represented in Fig. 5.

We now consider the system under illumination. Equations (14)–(16) in the steady state out of equilibrium become

$$\frac{dn}{dt} = G_L - U_1 - U_2 + U_3 + U_4 = 0 \ , \tag{14'}$$

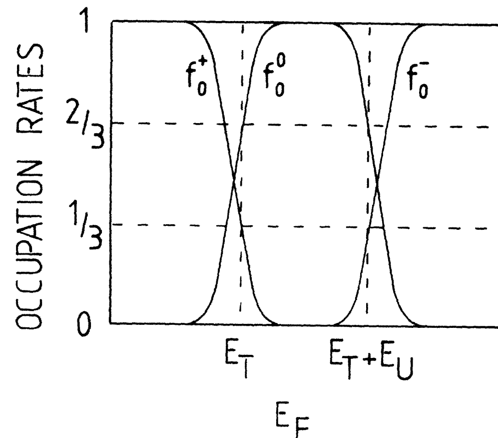

FIG. 5. Equilibrium occupation probabilities of dangling bonds in the T_3^+, T_3^0, and T_3^- states.

$$\frac{dp}{dt}=G_L-U_5-U_6+U_7+U_8=0\ , \qquad (15')$$

$$\frac{d[T_3^+]}{dt}=U_1+U_7-U_3-U_5=0\ . \qquad (16')$$

Substituting the expressions of the flows in Eqs. (14') and (15') allow us to express the probabilities under illumination f^+, f^0, and f^- as functions of n,p, and the capture or emission coefficients

$$f^+=\frac{1}{1+\frac{e_p^++nc_n^+}{e_n^0+pc_p^0}\left[1+\frac{e_p^0+nc_n^0}{e_n^-+pc_p^-}\right]}\ , \qquad (20)$$

$$f^0=\frac{1}{1+\frac{e_n^0+pc_p^0}{e_p^++nc_n^+}+\frac{e_p^0+nc_n^0}{e_n^-+pc_p^-}}\ , \qquad (21)$$

$$f^-=1-f^0-f^+\ . \qquad (22)$$

The rates of occupied electron and hole traps f_n and f_p can be obtained more easily. Due to the nature of trap levels, we have both at thermal equilibrium or under illumination

$$U_9=U_{10}\ , \qquad (23)$$

$$U_{11}=U_{12}\ . \qquad (24)$$

Assuming that the equilibrium trap-occupation rates f_n^0 and f_p^0 follow Fermi-Dirac statistics, we obtain from (23) and (24)

$$f_n=\frac{n}{n+n_i\exp[(E_{t_n}-E_i)/k_BT]}\ , \qquad (25)$$

$$f_p=\frac{n_i\exp[(E_i-E_{t_p})/k_BT]}{p+n_i\exp[(E_i-E_{t_p})/k_BT]}\ . \qquad (26)$$

The charge conservation between the equilibrium state and the illuminated state gives

$$n_0-p_0+N_Tf_0^0+2N_Tf_0^-+N_{t,n}f_n^0+N_{t,p}f_p^0$$
$$=n-p+N_Tf^0+2N_Tf^-+N_{t,n}f_n+N_{t,p}f_p\ . \qquad (27)$$

Replacing the expressions of f^0, f^-, f_n, and f_p given by (21), (22), (25), and (26) in (27), we obtain a fourth-degree equation which directly links n and p. Given an n (p) value, it is possible to obtain numerically p (n). Inserting n and p values in (14'), we obtain as in the preceding section a parametric representation for the photoconductivity σ_{ph} and the generation rate G_L.

III. CALCULATION RESULTS FOR RECOMBINATION AT DANGLING BONDS

A. Choice of parameters

Among the many parameters involved in Eqs. (17)–(19) and (20)–(23) which together with (9) and (11) are necessary to obtain a γ value, various quantities are already well known for a-Si:H and some values taken from the literature will be adopted. We shall retain only three variable DB parameters that are still subjects of controversy: the energy position of the T_3^0 state, the N_T concentration in low defect density a-Si:H and the ratio of the charged to neutral capture cross sections.

1. Fixed DB parameters

For the first class of parameters nearly identical values have been derived from experiments on glow-discharge a-Si:H in different laboratories. The effective densities of conduction- and valence-band states have been taken both equal to 10^{21} cm^{-3}. The thermal velocities were $v_n=v_p=10^7$ cm s^{-1}. A constant value of ~ 1.8 eV was taken for the optical gap of undoped and lightly doped material. Doing so, we neglect some variations between 1.7 and 1.85 eV occurring with phosphorus doping[28] and between 1.75 and 1.82 eV observed with low-boron-doping levels.[19] We derive the intrinsic value of carrier density $n_i=3\times10^5$ cm^{-3} at 300 K. The microscopic mobilities in the bands derived by Tiedje *et al.*[22] are 13 and 0.7 cm^{2}V^{-1}s^{-1} for electrons and holes, respectively. Because of the agreement among other estimates in the literature, the following values are adopted:

$$\mu_n=10\ \text{cm}^2\text{V}^{-1}\text{s}^{-1}\ \text{ and }\ \mu_p=1\ \text{cm}^2\text{V}^{-1}\text{s}^{-1}\ .$$

Another set of parameters that can be fixed relates to the DB characteristics on which there is general agreement between various laboratories. Two of them are the capture cross sections of the T_3^0 state for electrons (σ_n^0) and for holes (σ_p^0). The most accurate determinations of σ_n^0 and σ_n^0 result from the observation that the $\mu_d\tau N_T$ products are constant over several orders of magnitude of N_T.[29] Here μ_d and τ are the drift mobility and the effective lifetime of the majority carriers. Assuming that free carriers are captured by dangling bonds using a ballistic model, the capture cross sections are derived through relations of the type

$$\mu_d\tau N_T=\mu_n/\sigma_n^0v_n\ .$$

From $\mu_d\tau N_T$ products measured using time-of-flight transient photoconductivity, Street[6] derived

$$\sigma_n^0=4\times10^{-15}\ \text{cm}^2$$

and

$$\sigma_p^0=2\times10^{-15}\ \text{cm}^2\ .$$

From carrier collection length measurements in Schottky barriers, Abeles *et al.*[30] obtained $\sigma_p^0=1.3\times10^{-15}$ cm^2 in glow-discharge a-Si:H and Moustakas *et al.*[29] obtained $\sigma_p^0=6\times10^{-15}$ cm^2 for sputtered a-Si:H. Values between 2×10^{-16} and 5×10^{-15} cm^2 for σ_n^0 have also been derived from capacitance temperature analysis on Schottky diodes.[31] For the following calculations, the values were fixed at $\sigma_n^0=\sigma_p^0=3\times10^{-15}$ cm^2.

Finally, the effective correlation energy E_U has been measured through a variety of experiments and found to be equal to 0.4 eV from ESR (Ref. 7) or photothermal deflection spectroscopy (PDS) (Ref. 25), 0.5 eV from optical modulation spectroscopy[32] or 0.36 eV from temperature-modulated space-charge-limited currents (SCLC's).[33] We fix the value at 0.4 eV.

2. *Variable DB parameters*

Much more controversy surrounds the position of the E_T level within the energy gap. A theoretical calculation by Joannopoulos[34] placed it at 1.4 eV from the conduction band. This estimate agrees fairly well with optical measurements of PDS (Ref. 35) or optical modulation spectroscopy[32] which place it at 1.3 or 1.2 eV from E_c, respectively. Also consistent with this position is the placement of the T_3^- state at 0.85 eV from E_c by Cohen *et al.*[24] from DLTS and ESR results on an *a*-Si:H Schottky diode. However, other results disagree strongly with these. The T_3^- state is placed at 0.6 eV from ODMR,[36] 0.52 eV from isothermal capacitance transient spectroscopy[37] and 0.61 eV from temperature-modulated SCLC (Ref. 33) results. This set of values in turn agrees well with the result of Spear *et al.*[38] which places the T_3^0 state between 0.95 and 1 eV below E_c. To fix our limits of variation on the E_T position, we use the arguments given by Stuke and co-workers[39,40] that in *a*-Si:H, which contains a high density of dangling bonds, the stable position of the Fermi level must lie half way between the T_3^0 and the T_3^- levels. In undoped *a*-Si:H, where dangling bonds have been created by illumination or by electron irradiation,[40] a constant value of 0.85 eV has been derived for the bulk conductivity activation energy. Even allowing E_U to vary between 0 and 0.5 eV, the T_3^0 level would be expected to lie in the range 0.85—1.1 eV below E_c. That is the range we shall accept for our variations of E_T expressed as $E_i - 0.2$ eV, $E_i + 0.1$ eV taking $E_i = E_G/2 = 0.9$ eV.

Dangling-bond concentrations can vary over orders of magnitude depending on the deposition parameters or posttreatments and can be directly measured by ESR absorption. The detection limit of the technique is about 10^{16} cm^{-3} for a 1-μm-thick *a*-Si:H film so that, in low-defect-density *a*-Si:H, N_T is usually determined by indirect measurements. The lowest values are between 3×10^{15} cm^{-3} (Refs. 30 and 35) and 5×10^{14} cm^{-3}.[23,41] Here we take 10^{14} cm^{-3} as a lower limit.

The capture cross sections of the charge states T_3^+ and T_3^- determine the coefficients e_p^+, c_n^+, e_n^-, and c_p^- in Eqs. (20) and (21). We shall simplify the problem by choosing a unique value for the ratio of the charge-to-neutral-state capture cross sections: $\sigma_n^+/\sigma_n^0 = \sigma_p^-/\sigma_p^0 = r$. The Coulombic center is much more efficient in trapping a carrier than the neutral one leading to $r \gg 1$ with r values between 10 and 1000.[42] In *a*-Si:H, a value of 5 has been reported by Street and co-workers[6,41] while the results of Spear *et al.*[43] agree better with $r \gtrsim 30$. In our model, r will be allowed to vary between 5 and 50.

3. *Trapping parameters*

Realistic trap depths for electrons and holes are given by the drift mobility activation energies, measured by the time-of-flight technique. The values have decreased over the last years probably due to improved material quality. For electrons, thermal activation energies of 0.13 eV (Ref. 44) and 0.10 eV (Ref. 45) have been obtained recently while much higher values between 0.3 and 0.4 eV (Refs. 41 and 45) are given for holes. These activation energies are generally interpreted as multiple trapping in band-tail states and thermal release into the bands. Within our simplified trapping picture, they would correspond to the $E_0 - E_{t,n}$ and $E_V - E_{t,p}$ distances which are fixed at 0.1 and 0.3 eV, respectively, in the following. Finally, the trap concentrations will be allowed to vary between 0 and 10^{19} cm^{-3}.

B. Calculation of results and comments

1. *Variations of photoconductivity and occupation statistics with photogeneration rate*

The parametric representation described in Sec. II B allows the determination of $\sigma(x)$ as a function of the photogeneration rate $G_L(x)$ and the effective photoconductivity of a film (thickness e) is calculated as a function of photon flux ϕ, according to the relation in the Appendix. Typical variations are given in Fig. 6 for a single set of parameters,

$$N_T = 5\times10^{15}\ \text{cm}^{-3},\quad E_T - E_i = -0.05\ \text{eV},\quad r = 50\ ,$$

no trapping, and two positions of the Fermi level. Generally a nearly straight line is obtained [Fig. 6(a)] which allows the unambiguous determination of a γ value. In some cases, the σ_{ph} versus G_L curve shows a kink [Fig. 6(b)] and two γ values can be defined according to the G_L range. It is therefore very important to assign a value of photogeneration rate to a photoconductivity exponent. We shall consider G_L in the range of 10^{16}—10^{19} which corresponds to experimental conditions of incident photon fluxes between 10^{12} and 10^{15} cm^{-2} s^{-1} for energy of 2 eV.

The variations in the occupation rates of the three charge states are given in Figs. 7(a) and 7(b) for the two cases of Fig. 6 where f^0 is close to 1 at equilibrium. Over the whole G_L range, only a very small variation of the T_3^+, T_3^0, and T_3^- rates is observed. For example, in Fig. 7(b), at $G_L < 10^{16}$ cm^{-3} s^{-1}, the dangling bonds are statistically in the same states as in the dark. A second re-

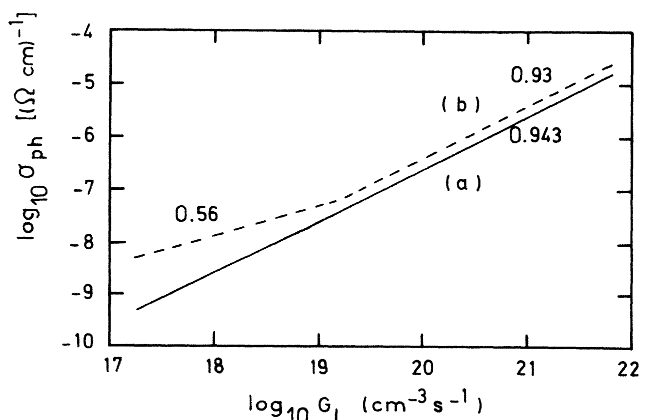

FIG. 6. Dependence of photoconductivity on photogeneration rate for recombination at dangling bonds: (a) $E_F - E_i = 0$ eV; (b) $E_F - E_i = 0.12$ eV.

gime of occupation is established at $G_L > 10^{18}$ cm^{-3}s^{-1} corresponding to a new stable quasiequilibrium point between the three charge states of which only 2% of the T_3^0 states have been converted into T_3^+ and T_3^-. This is because the free-carrier concentrations remain well below the value of N_T so the relation (27) is satisfied without any large change in the charge distribution of the dangling bonds. The transition between the two regimes at $G_L \simeq 10^{18}$ cm^{-3}s^{-1} gives rise to the kink in the σ_{ph} versus G_L curve of Fig. 6(b). Similar curves are obtained in the presence of trap levels of densities $N_{t,n} = N_{t,p} = 10^{19}$ cm^{-3} and we have observed the same relative variations of occupation for the case where f^+ is close to 1 as in p-type a-Si:H. The present analysis shows that in these cases a weak light-induced ESR signal is expected.

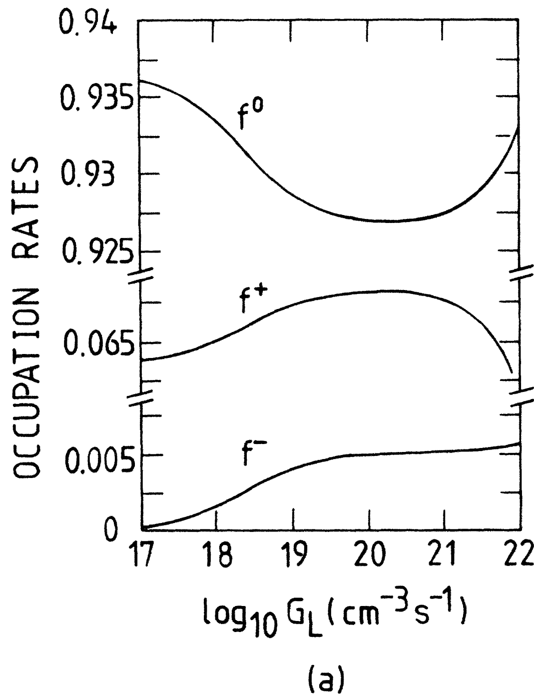

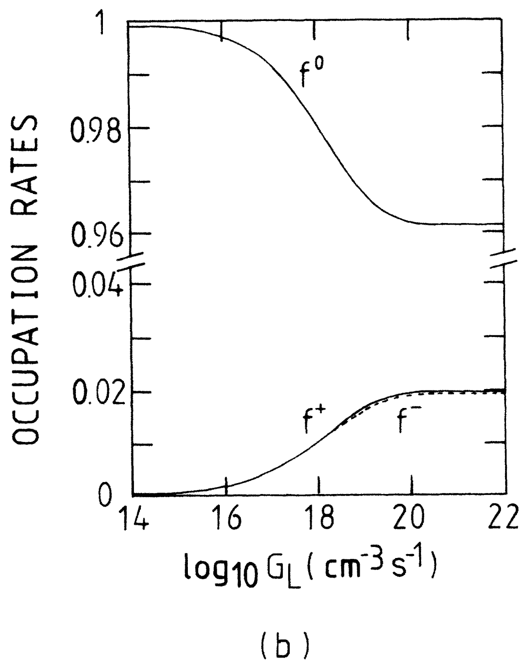

FIG. 7. Occupation probabilities of the DB states under illumination for the two cases of Fig. 6.

2. Fermi-level effects on the exponent γ

We calculated γ versus E_F plots for various values of N_T, E_T, trapping, and r. The variations of E_F with regard to E_i reproduced the experimental moderate p and n doping. The photon flux range for γ determination was between 10^{12} and 10^{15} photons cm^{-2}s^{-1}. Figure 8 shows the $\gamma(E_F)$ curves calculated for different N_T densities with the fixed parameters $E_T = -0.05$ eV, $r = 50$, $N_{t,n} = N_{t,p} = 0$. Oscillations between 0.5 and 1 are systematically obtained with $\gamma = 0.5$ for E_F at -0.3 and $+0.3$ eV from E_i. For E_F around E_T, $\gamma = 1$ and there is an intermediate minimum with E_F at $E_T + 0.2$ eV that decreases down to 0.5 when N_T increases. The analogy with the single level model treated in Sec. II A is obvious. First, the $\gamma = 1$ plateau appears at $E_T + 0.4$ eV which corresponds to the position of the T_3^- level. In some way, the two-correlated-level system behaves like a set of two independent levels as long as E_F remains out of the $[E_T, E_T + E_U]$ range. In particular, we note here for p-type photoconductivity, when, for example, at $E_F = -0.2$ eV, the exponent γ goes from 0.59 to 1 as N_T is increased from 10^{14} to 5×10^{16} cm^{-3}. High-N_T densities tend to yield $\gamma = 1$ over a wider range of E_F positions.

We now consider the $\gamma(E_F)$ curves of Fig. 9 obtained with $N_T = 5\times10^{15}$ cm^{-3}, where the E_T position varies between -0.2 and $+0.1$ eV while the other quantities remain unchanged. The common feature to all curves is that $\gamma = 1$ when $E_F = E_T$ and γ has a minimum at

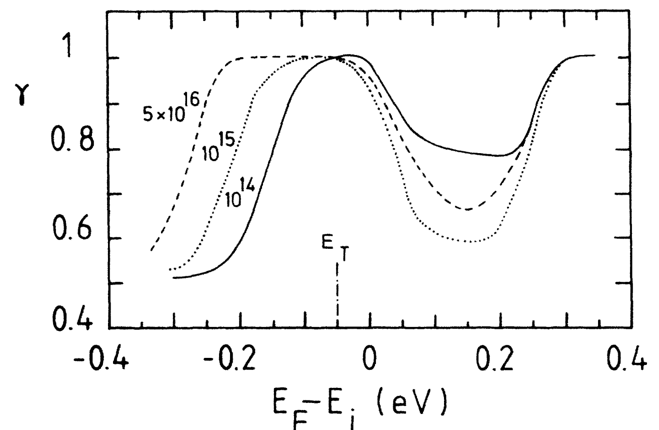

FIG. 8. Variation of the exponent γ vs E_F at different N_T.

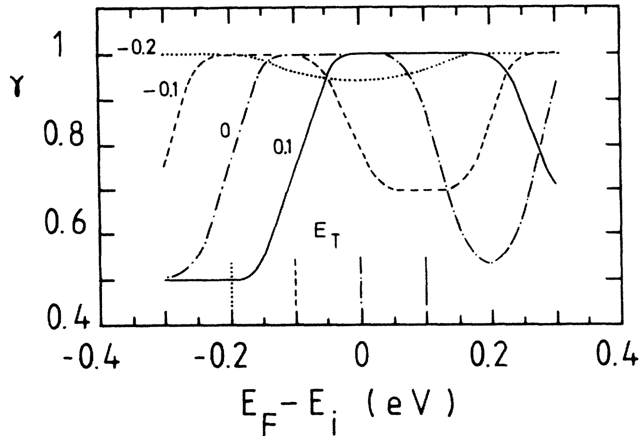

FIG. 9. Variations of γ vs E_F curves for different positions of the T_3^0 level. The E_T positions and draw types are indicated by the bars on the abscissa.

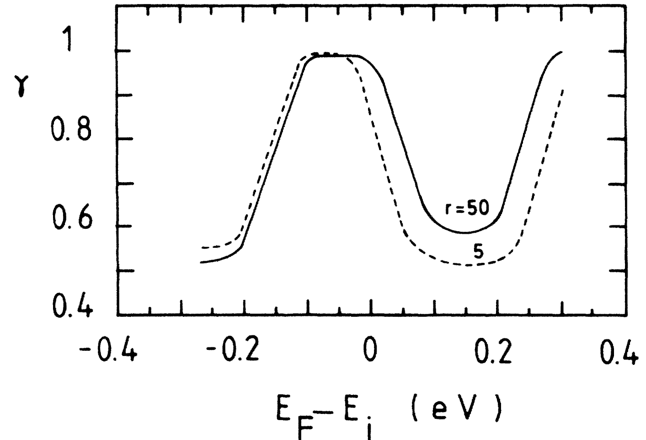

FIG. 11. Influence of the σ^+/σ^0 ratio on the γ vs E_F variations.

$E_T+0.2$ eV, i.e., $E_T+E_U/2$. The symmetry of the curve with respect to E_T and the amplitude of the dip at $E_T+E_U/2$ are progressively weaker with the lowering of E_1, where for $E_T=-0.2$ eV, γ varies only between 1 and 0.89.

The effect of trapping is illustrated by Fig. 10. The $\gamma(E_F)$ curves have been calculated for different trap densities: $N_T=5\times10^{15}$ cm^{-3}, $E_T=-0.05$ eV. In the E_F range shown, trapping has little effect on the $\gamma(E_F)$ curve except for E_F in the lower part of the gap where the transition from 0.5 to 1 is shifted to higher energies as the hole trap densities increase. In other words, hole trapping tends to decrease γ to 0.5 for p-type photoconductivity, as predicted by all photoconductivity models of a-Si:H. However, the same γ values were obtained in this E_F region for $N_{t,n}=10^{17}$ and $N_{t,n}=10^{19}$ cm^{-3}.

Finally we show the effect of the charge-to-neutral state cross-section ratio r in Fig. 11. The two curves have been calculated with $r=5$ and $r=50$ with other parameters fixed: $N_T=5\times10^{15}$ cm^{-3}, $E_T=-0.05$ eV, $N_{t,n}=N_{t,p}=10^{19}$ cm^{-3}. Obviously this parameter affects the $\gamma(E_F)$ curves in the E_F region between E_T and E_t+E_U where dangling bonds are in the T_3^0 state at equilibrium. Higher γ values are obtained when the capture of an electron (a hole) by a T_3^+ state (T_3^-) is much easier than the corresponding captures by a T_3^0 state.

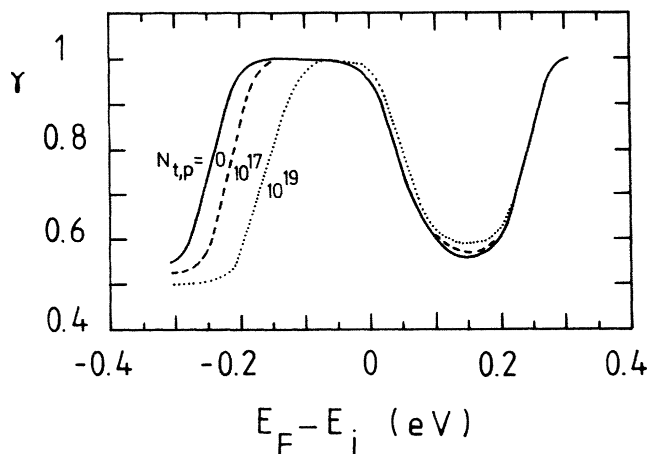

FIG. 10. Effect of trapping on the γ vs E_F curves.

IV. DISCUSSION

The predictions of our model could be tested experimentally in detail if one could prepare a-Si:H samples having controlled densities N_T, $N_{t,n}$, and $N_{t,p}$ and in which the E_F positions could be adjusted. Unfortunately, these quantities change together irrespective of the deposition process of a-Si:H. Nevertheless, we would like to emphasize that the general trends observed experimentally for a-Si:H agree with the conclusions of the model presented here. A few of these have been selected for discussion: photoconductivity of lightly-boron-doped a-Si:H, quenching of ESR and LESR.

A. Experimental $\gamma(E_F)$ from light-boron doping

Boron doping of glow-discharge a-Si:H at nominal ratios of B_2H_6 to SiH_4 between 0 and 100 ppm has been carried out in this laboratory in a study of the properties of lightly n- or p-type materials. In this range, E_F moves from $+0.24$ to -0.30 eV from E_i as indicated by the activation energies of dark conductivity. PDS results indicate no significant increase in gap state densities up to 10-ppm doping ($E_F-E_i=-0.25$ eV) so that, to a good approximation, E_F is shifted in the central region of the gap through a constant DOS. The detailed results have been published elsewhere[19] and we shall present only the results in Fig. 12 where the variations of γ measured with 2-eV photons for incident fluxes between 10^{12} and 10^{15} photons cm^{-2} s^{-1}, is presented. The error in the E_F position is about 20 meV except for the intrinsic samples where mixed conduction and nonlinear $\log_{10}\sigma(1/T)$ curves resulted in an uncertainty of ±0.05 eV represented

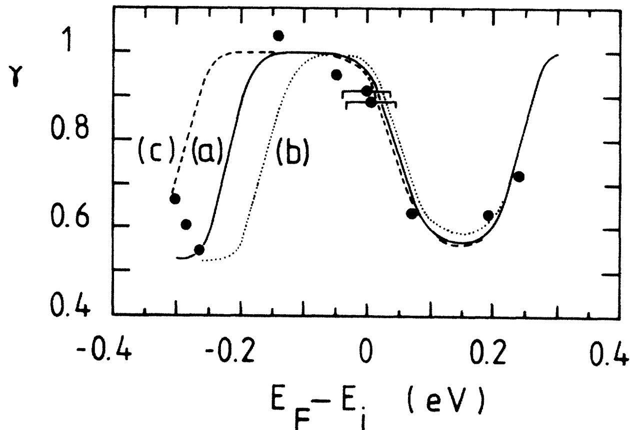

FIG. 12. Experimental variations of the exponent γ versus Fermi-level position in lightly-boron-doped glow discharge a-Si:H compared to theory: ●, experimental points; (a) $N_T=5\times10^{15}$ cm^{-3}, $N_{t_p}=10^{17}$ cm^{-3}; (b) $N_T=5\times10^{15}$ cm^{-3}, $N_{t_p}=10^{19}$ cm^{-3}; (c) $N_T=5\times10^{16}$ cm^{-3}, $N_{t_p}=10^{19}$ cm^{-3}.

by the bars in Fig. 12. The shape of the experimental curve agrees with the general theoretical behavior. Good fits are obtained in the figure although it is not possible to fix a unique set of parameters because of the limited data between -0.1 and -0.25 eV and the symmetrical offsets of N_T and $N_{t,p}$ on the γ transition from 1 to 0.5 in this region.

The gap defect density, measured by PDS, is about 5×10^{16} cm^{-3} while the dark ESR measurements on undoped and slightly n-type samples indicated $N_T<10^{16}$ cm^{-3}. The difference between ESR and PDS results must be attributed to other optically active defects besides dangling bonds.[46] If we take $N_T=5\times10^{15}$ cm^{-3}, good agreement is obtained with $N_{t,p}=10^{17}$ cm^{-3} (full line of Fig. 12) and any value for $N_{t,n}$ since electron trapping has no effect in the range studied. Other parameters are chosen to fit the dip around 0.1 eV with reasonable accuracy. The best-fit yield, $E_T=-0.05$ eV, $r=50$, while position of the minimum agrees well with $E_U=0.4$ eV. The situation of the T_3^0 level at 0.95 eV from E_c and other deduced values are in close agreement with the results of Spear *et al.*[38]

B. Exponent γ at intermediate doping

Studies on P and B doping have markedly shown that gap defects are created when dopant atoms are incorporated into a-Si:H. First, deep defects identified as dangling bonds[23,24,35,47] are created and their density depends on the dopant concentration N_D according to a law: $N_T\propto N_D^{1/2}$.[47] Corresponding changes in the Urbach slope are seen by PDS (Ref. 35) indicating that tail state densities also increase. In the simplest picture, substitutional dopants also introduce donor and acceptor states near the band edges which may act as shallow traps. From this model we expect the transitions to $\gamma=0.5$ to occur at high doping only if $N_{t,n}$ ($N_{t,p}$) increases faster than N_T.

The three left-hand side points of Fig. 12 corresponding to the 10—100-ppm diborane concentrations show a somewhat different behavior: in this range, γ increases from 0.55 (10 ppm) to 0.67 (100 ppm). The calculated theoretical curves suggest an increase of the DB density rather than a change in $N_{t,p}$ concentration. The case of high doping will not be discussed here as the simple description developed in Sec. II B does not apply when E_F enters the band tails. True exponential trap distributions should be considered and those equations are not easily solved.

C. ESR under illumination

The most striking prediction of the model is that it is impossible to invert the equilibrium occupation statistics upon illumination of a-Si:H. A thorough search of the literature shows that ESR experiments under illumination qualitatively agree with this conclusion.

The dangling-bond ESR signal at $g=2.0055$ disappears in doped a-Si:H and can be observed under light excitation (LESR) below 200 K.[48] No signal can be detected at room temperature in agreement with our calculations which are strictly valid at 300 K.

The difficulty of inverting occupation statistics still remains when LESR measurements are performed at 30 K, as in the work of Street *et al.*[47] The determination of dangling-bond concentration from the LESR intensity was shown to lead to important underestimations of DB densities compared to other values deduced from PDS (Ref. 35) for photoluminescence.[47] This is well illustrated in Fig. 17 of their paper. In the same way, Friederich and Kaplan[49] have reported on the quenching of ESR signal at 100 K in undoped a-Si:H. Their results summarized in Fig. 5 of Ref. 49 can be fitted by a simple law indicating that the ESR intensity is reduced only by 10% when an illumination intensity of 10^{18} photons cm^{-2} s^{-1} is applied.

We can say that the theoretical results of Fig. 7 explain the absence of optically induced DB signal at 300 K. Experimental ESR or LESR results at low temperature also agree qualitatively with the prediction of the model although quantitative analysis for recombination at DB's must still be done.

V. CONCLUSIONS

In conclusion, we have developed a model for the recombination at dangling bonds in a-Si:H and steady-state photoconductivity. In addition, the statistics of the three charge states of the recombination centers have been calculated as a function of the photogeneration rate. The theoretical variations of the exponent γ versus the Fermi-level position in a-Si:H have been analyzed taking into account the effects of dangling bonds and trap densities, energy position of the singly occupied state, and the ratio of charge-to-neutral capture cross sections. In agreement with experimental data, we have shown the following.

(i) Steady-state photoconductivity and dangling-bond occupation statistics are primarily determined by the dark equilibrium occupation statistics.

(ii) The occupation probabilities are hardly modified by illumination leading to weak quenching of ESR in un-

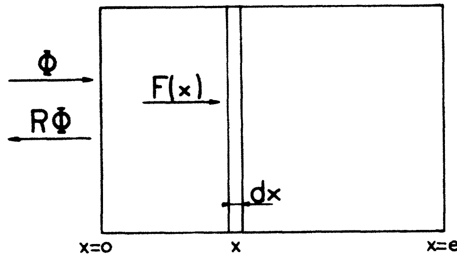

FIG. 13. Absorption in the thickness of the film.

doped a-Si:H and weak LESR signals in doped a-Si:H at 300 K.

(iii) The changes in the photoconductivity exponent between 0.5 and 1 with the position of E_F are consistent with a position of the T_3^0 level at $E_i - 0.05$ eV, i.e., 0.95 eV from E_c, an effective correlation energy of 0.4 eV and $\sigma^+/\sigma^0 = 50$.

We are currently improving the model in order to simulate the temperature dependence of the photoconductivity. Another possible extension of this model could be to apply it to photoconductive amorphous semiconductors with negatively correlated defects.

ACKNOWLEDGMENTS

We wish to thank E. Bustarret and A. Deneuville for a critical reading of our manuscript. This work was supported by the "Programme Interdisciplinaire de Recherche sur les Energies Nouvelles-Association Française pour la Maîtrise de l'Energie" under the "Arc Silicium Amorphe project." One of us (F.V.) has benefitted from the financial support of the Saint-Gobain Company. The Laboratoire d'Etudes des Propriétés Electroniques des Solides is "associated to" Université Scientifique, Technologique et Médicale de Grenoble."

APPENDIX: EFFECT OF THICKNESS ON THE PHOTOCONDUCTIVITY

If we call $F(x)$ the photon flux at a distance x from the front of the film, the photogeneration rate $G(x)$ at this point is equal to $\eta\alpha(x)F(x)$ where $\alpha(x)$ is the optical absorption and η the quantum yield (Fig. 13). Assuming $\eta = 1$ and α independent of the position in the bulk, $G_L(x) = \alpha F(x)$. Calling Φ the photon flux which enters the film and R the reflection of the interface: $F(x) = \Phi(1-R)e^{-\alpha x}$. If we admit that the photoconductivity γ does not vary a lot in the bulk, as is shown in Sec. III B 1, the photoconductivity at x, $\sigma(x)$, is equal to $K[G_L(x)]^\gamma$. Consequently, the effective photoconductivity σ_{eff} of the film in coplanar geometry is

$$\sigma_{\mathrm{eff}} = \frac{1}{e}\int_{x=0}^{x=e} \sigma(x)dx = K\frac{1-e^{-\alpha\gamma e}}{\alpha\gamma e}\alpha^\gamma(1-R)^\gamma\Phi^\gamma .$$

The effect of the thickness of the film on the photoconductivity is a function $(1-e^{-\alpha\gamma e})/\gamma e$ which can be different to the classical expression $(1-e^{-\alpha e})/e$ if $\gamma \neq 1$.

[1]R. A. Street, Adv. Phys. **30**, 593 (1981).
[2]B. A. Wilson, A. M. Sergent, and J. P. Harbison, Phys. Rev. B **30**, 2282 (1984).
[3]R. A. Street, D. K. Biegelsen, and R. L. Weisfield, Phys. Rev. B **30**, 5861 (1984).
[4]K. Morigaki, Y. Sano, and I. Hirabayashi, Solid State Commun. **39**, 947 (1981).
[5]T. D. Moustakas, C. R. Wronski, and T. Tiedje, Appl. Phys. Lett. **39**, 721 (1981).
[6]R. A. Street, Appl. Phys. Lett. **41**, 1060 (1982).
[7]H. Dersch, J. Stuke, and J. Beichler, Phys. Status Solidi B **105**, 265 (1981).
[8]R. A. Street and D. K. Biegelsen, J. Non-Cryst. Solids **35/36**, 651 (1980).
[9]L. Schweitzer, M. Brunewald, and H. Dersch, J. Phys. (Paris) Colloq. **C4-42**, 827 (1981).
[10]For a review, see for example, R. S. Crandall, in *Semiconductors and Semimetals,* edited by J. I. Pankove (Academic, New York, 1984), Vol. 21B, p. 245.
[11]D. A. Anderson and W. E. Spear, Philos. Mag. **36**, 695 (1977).
[12]C. R. Wronski and R. E. Daniel, Phys. Rev. B **23**, 794 (1981).
[13]T. Kagawa, N. Matsumoto, and K. Kumabe, Phys. Rev. B **28**, 4570 (1983).
[14]E. Arene and J. Baixeras, Phys. Rev. B **30**, 2016 (1984).
[15]A. Rose, *Concepts in Photoconductivity and Allied Problems* (Interscience, New York, 1963).
[16]M. Hack, S. Guha, and M. Shur, Phys. Rev. B **30**, 6991 (1984).
[17]H. Okamoto, H. Kida, and Y. Hamakawa, Philos. Mag. **49**, 231 (1984).
[18]W. Shockley and W. T. Read, Phys. Rev. **87**, 835 (1952).
[19]D. Jousse, C. Chaussat, F. Vaillant, J. C. Bruyere, and F. Lesimple, J. Non-Cryst. Solids **77/78**, 627 (1985).
[20]B. Hoheisel, R. Fischer, and J. Stuke, J. Phys. (Paris) Colloq. **C4-42**, 819 (1981).
[21]See for example, H. Fritzsche, J. Non-Cryst. Solids **77/78**, 273 (1985); also see Ref. 6, Cohen *et al.*, in Ref. 24, and Spear *et al.* in Ref. 38.
[22]T. Tiedje, J. M. Cebulka, D. L. Morel, and B. Abeles, Phys. Rev. Lett. **46**, 1425 (1981).
[23]D. V. Lang, J. D. Cohen, and J. P. Harbison, Phys. Rev. B **25**, 5285 (1982).
[24]J. D. Cohen, J. P. Harbison, and K. W. Wecht, Phys. Rev. Lett. **48**, 109 (1982).
[25]W. B. Jackson, Solid State Commun. **44**, 477 (1982).
[26]C. T. Sah and W. Shockley, Phys. Rev. **109**, 1103 (1958).
[27]H. Okamoto and Y. Hamakawa, Solid State Commun. **24**, 23 (1977).
[28]C. R. Wronski, B. Abeles, T. Tiedje, and G. D. Cody, Solid State Commun. **44**, 1423 (1982).
[29]T. D. Moustakas, C. R. Wronski, and T. Tiedje, Appl. Phys. Lett. **39**, 721 (1981).
[30]B. Abeles, C. R. Wronski, Y. Goldstein, and G. D. Cody, Solid State Commun. **41**, 251 (1982).
[31]D. Jousse and S. Deleonibus, J. Appl. Phys. **54**, 4001 (1983).
[32]Z. Vardeny and J. Tauc, Phys. Rev. Lett. **54**, 1844 (1985).
[33]J. Kocka, O. Stika, I. Kubelik, M. Vanecek, A. Triska, F. Schauer, and O. Zmeskal, J. Non-Cryst. Solids **77/78**, 385

(1985).

[34]J. D. Joannopoulos, J. Non-Cryst. Solids **35/36**, 781 (1980).

[35]W. B. Jackson and N. M. Amer, Phys. Rev. B **25**, 5559 (1982).

[36]K. Morigaki, Y. Sano, I. Hirabayashi, M. Konagai, and M. Suzuki, Solid State Commun. **43**, 751 (1982).

[37]H. Okushi, T. Takahama, Y. Tokumaru, S. Yamasaki, H. Oheda, and T. Tanaka, Phys. Rev. B **27**, 5184 (1983).

[38]W. E. Spear, H. L. Steemers, P. G. Lecomber, and R. A. Gibson, Philos. Mag. B **50**, 133 (1984).

[39]J. Stuke, in *Poly-micro-crystalline and Amorphous Semiconductors,* edited by P. Pinard and S. Kalbitzer (Editions de Physique, Paris, 1984), p. 415.

[40]H. Dersch, L. Schweitzer, and J. Stuke, Phys. Rev. B **28**, 4678 (1983).

[41]R. A. Street, J. Zesch, and M. J. Thompson, Appl. Phys. Lett. **43**, 672 (1983).

[42]C. H. Henry and D. V. Lang, Phys. Rev. B **15**, 989 (1977).

[43]W. E. Spear, A. C. Hourd, and S. Kinmond, J. Non-Cryst. Solids **77/78**, 607 (1985).

[44]W. E. Spear, H. L. Steemers, and H. Mannsperger, Philos. Mag. B **48**, L49 (1983).

[45]J. M. Marshall, R. A. Street, and M. J. Thompson, Phys. Rev. B **29**, 2331 (1984).

[46]E. Bustarret, D. Jousse, C. Chaussat, and F. Boulitrop, J. Non-Cryst. Solids **77/78**, 295 (1985).

[47]R. A. Street, D. K. Biegelsen, and J. C. Knights, Phys. Rev. B **24**, 969 (1981).

[48]D. K. Biegelsen and J. C. Knights, in *Amorphous and Liquid Semiconductors,* edited by W. E. Spear (University of Edinburgh, Edinburgh, Scotland, 1977), p. 429.

[49]A. Friederich and D. Kaplan, J. Non-Cryst. Solids **35/36**, 657 (1980).